13 HYDROGEOPHYSICAL CASE STUDIES AT THE LOCAL SCALE: THE SATURATED ZONE

DAVID HYNDMAN[1] AND JENS TRONICKE[2]

[1]*Dept. of Geological Sciences, Michigan State University, East Lansing, Michigan 48824, U.S.A.*

[2]*Institute of Geophysics, Swiss Federal Institute of Technology, ETH-Hoenggerberg, CH-8093 Zurich, Switzerland*

13.1 Introduction

Modern geophysical methods provide significant promise for estimating subsurface aquifer properties of the saturated zone in a minimally invasive manner. Mapping aquifer boundaries and internal stratification, estimating spatial distribution of hydrogeologic parameters, or monitoring tracer and contaminant plumes are examples of geophysical tools successfully applied. A general benefit of geophysical methods is the ability to collect high-resolution data in the horizontal dimension, where core/borehole data is nearly always limited. The complementary nature of core/borehole data and 2-D or 3-D geophysical data promises to help improve the accuracy and resolution of aquifer characterization at a variety of scales. However, one significant remaining difficulty is transforming geophysical parameters into flow and transport properties. A series of approaches and petrophysical models have been developed to help in this transformation (e.g., see Chapter 4 and Chapter 9 of this volume), but often complex and non-unique parameter relationships complicate data analysis and interpretation.

The uncertain and potentially non-unique relation between geophysical and hydrogeologic properties is one of the main reasons that geophysical data are not regularly used to estimate hydrogeologic properties (such as hydraulic conductivity). There is little reason to expect a fundamental relation between these properties (e.g., seismic velocities do not directly depend on the ability of sediment to transmit fluids). For particular frequencies of seismic energy, however, the ability of fluids to flow is important to the stiffness of the media, which is related to seismic velocity and attenuation (Bourbie et al., 1987). The effect of fluid moving through pores to accommodate the stress imposed by a sound wave was also explored by Dvorkin et al. (1995) as an alternative to Biot theory. Estimating the relation between geophysical and hydrogeologic parameters is a site-specific endeavor, since no general relation is expected.

This chapter provides an overview of several recent case studies that use geophysical information to characterize aquifers at the scale of typical contaminant site investigations, or the "local" scale. The chapter focuses on seismic and ground-penetrating radar (GPR) methods for different saturated zone hydrogeological objectives, although a few electrical-method examples are mentioned. Several of the

Y. Rubin and S.S. Hubbard (eds.), Hydrogeophysics, 391–412.

presented examples demonstrate the application of individual geophysical techniques for specific hydrogeologic problems, while others integrate multiple geophysical datasets as well as geophysical and hydrogeologic information.

As was described in Chapter 1 of this volume, geophysical methods have been applied to solve several classes of subsurface problems. One of the most common classes involves inferring stratification or general structural properties. This can be achieved via surface reflection seismic and GPR techniques as well as electrical methods, depending on the scale and depth of interest. The goal of such methods is commonly to map the geologic architecture of the aquifer, which can be used to help generate a hydrostratigraphic model that better explains hydrologic observations or processes. A second class of methods focuses on estimating hydrogeologic aquifer parameters, such as hydraulic conductivity and porosity, using geophysical measurements constrained by hydrologic data. Many of these approaches rely on petrophysical relationships to transform geophysical properties into hydrogeologic properties. This class also includes the estimation of spatial correlation structures from geophysical data. A third class of methods attempts to map temporal variations in subsurface geochemistry. This can be especially enlightening at sites where point-source contaminants have a geophysical signature that differs from the surrounding fluids. This class of methods also involves dynamic imaging of tracer or contaminant movement to estimate aquifer properties. Such methods are especially well suited to estimate hydrogeologic properties in the subsurface, because time-lapse estimates of solute movement are more easily related to aquifer hydraulic properties than static measurements. A final class deals with studying appropriate aquifer analog sites (e.g., in gravel pits or quarries). Such studies aim to explore the potential of geophysical tools in different environments, e.g., by comparing the geophysical results to closely located outcrops. Below, we review these classes of geophysical investigation, using specific illustrative case studies.

13.2 Structural Characterization of Aquifers

A variety of geophysical techniques can provide important information about subsurface architecture. For example, electrical and electromagnetic methods have successfully distinguished between different subsurface lithologies (e.g., Pellerin, 2002), and detailed gravity surveys have been used to estimate depth to bedrock (e.g., Kick, 1985). Although these techniques can also be applied at the local scale, their main field and strength of application is found at larger scales (cf. Chapter 12 of this volume and Ward, 1990). Thus, these techniques are not discussed in detail here.

An important step toward defining aquifer hydraulic parameters is identifying a site's stratigraphic zonation, as well as important interfaces such as the water table. For such purposes, seismic and GPR techniques are often used, although other methods such as DC resistivity (e.g., Baines et al., 2002; Yaramanci et al., 2002) can also be used for this purpose. Within the last decade, a number of successful studies have been published that provide detailed two- or three-dimensional insights into the subsurface zonation and stratigraphy of different depositional environments using seismic (e.g., Miller et al., 1990; Büker et al. 2000; Baker et al., 2000; Jarvis and Knight, 2002) or

GPR reflection methods (e.g., Beres and Haeni, 1991; Smith and Jol, 1992; Beres et al., 1995; Young and Sun, 1996; McMechan et al., 1997; Tronicke et al., 1999; Lesmes et al., 2002; Lunt et al., 2003). Applying these techniques to characterize a specific site clearly requires consideration of both technical and physical limitations of such approaches in the environment of interest (cf. Chapters 7 and 8 of this volume). As an example, Figure 13.1 illustrates the potential of high-resolution 3-D GPR surveying for delineating subsurface stratigraphic features of saturated Quaternary deposits in the Reuss delta, Switzerland (Nitsche et al., 2002). In this example, “time slices” (which can be easily converted to “depth slices” for a homogenous or layered subsurface velocity distribution) from a 3-D data cube show prominent channel structures. At this site, total penetration depths of ~10 m were achieved using GPR antennas with a nominal center frequency of 100 MHz, in an environment where the water table was located ~1 m below ground surface. Such a depth of investigation is common for 100 MHz GPR surveys in gravel- and sand-dominated sites.

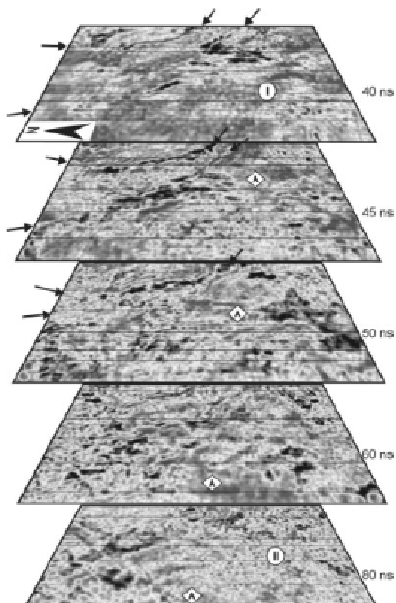

Figure 13.1. Example of detailed stratigraphic features obtained using 3-D GPR surveying (adapted from Nitsche et al., 2002). Time slices were extracted from a 3-D data cube covering a total area of 80 × 40 m, located in saturated Quaternary deposits of the Reuss delta, Switzerland. Arrows identify boundaries of prominent channel structures and labels identify characteristic radar units as interpreted by Nitsche et al. (2002).

For detailed stratigraphic analysis and interpretation, concepts of seismic and radar facies analysis have been developed (e.g., Sangree and Widmier, 1979; Beres and Haeni, 1991; Huggenberger, 1993; Beres et al., 1999; Regli et al., 2002; Lunt et al., 2003). As an example, Figure 13.2 shows a radar facies chart compiled by van Overmeeren (1998) for various sedimentary depositional environments in The Netherlands. This figure shows characteristic patterns obtained for several common sedimentological settings. Such a collection of representative reflection patterns allow researchers and practitioners to identify sedimentary sequence types and help distinguish, for example, between glacial and aeolian settings.

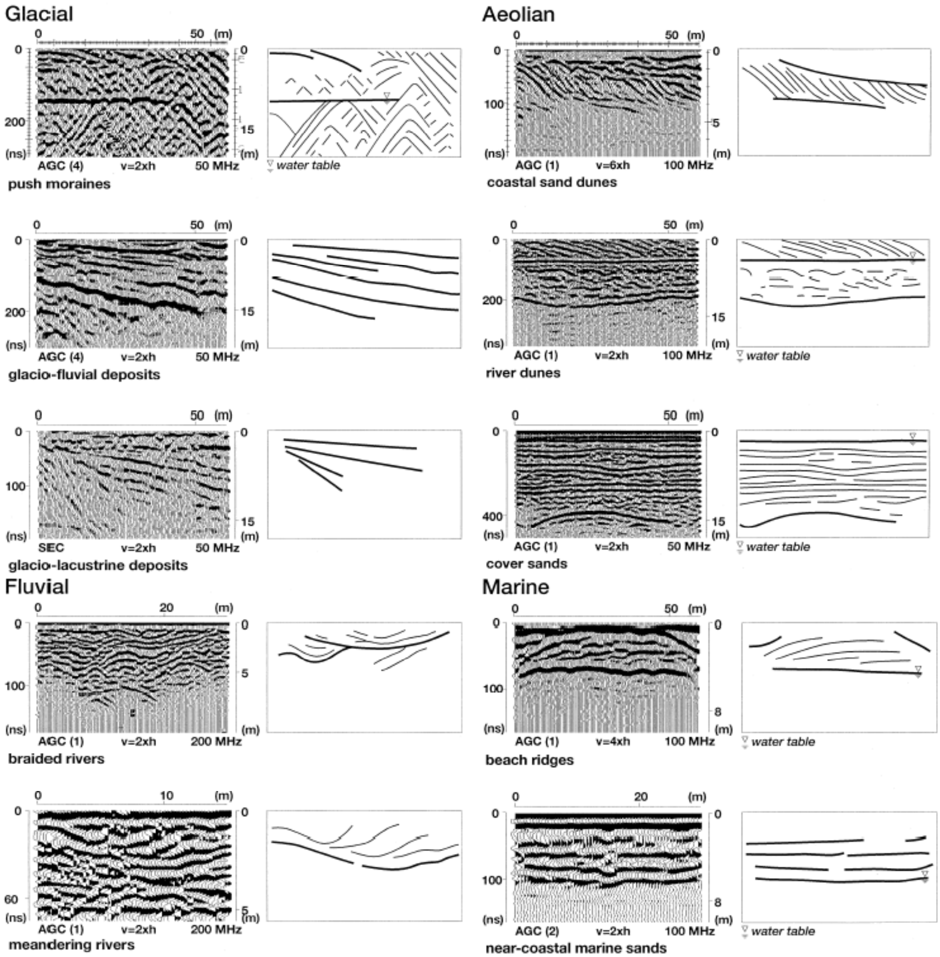

Figure 13.2. Radar facies chart for various characteristic sedimentary environments in The Netherlands (modified after van Overmeeren, 1998)

In many cases, the geometry of lithologic zones (e.g., sand, gravel, or clay) is the most important information that can be provided from a geophysical survey. Hyndman and Harris (1996) parameterized a crosswell seismic inversion, using a limited number of velocity values, to estimate the geometry of the primary lithologies for the shallow Kesterson aquifer in California's San Joaquin Valley (Figure 13.3). The approach used for this site simultaneously inverts travel times between all available well pairs for the spatial distribution of a limited number of seismic slowness (the reciprocal of seismic velocity) populations. This method can provide images that capture the dominant scale of subsurface heterogeneity, which can be an advantage over common tomographic parameterizations that provide smooth slowness fields, but can be difficult to translate into hydrogeologic parameters. The hydrogeologic properties for the estimated zones can then be inferred from core data, hydraulic testing, or some type of pump test or tracer test inversion.

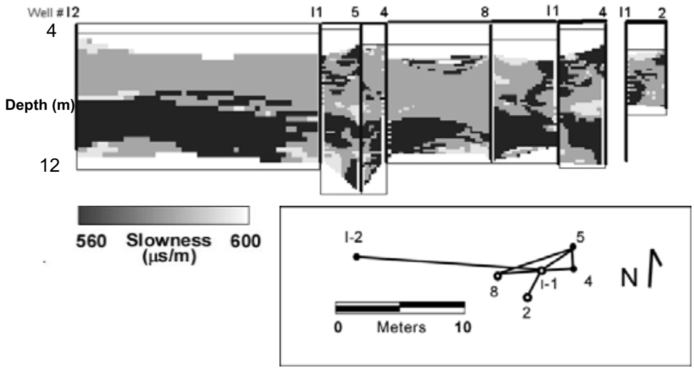

Figure 13.3. Zonal estimates of seismic slowness for the Kesterson site in California's San Joaquin Valley, developed using the multiple-population-inversion approach of Hyndman and Harris (1996)

Zonal geophysical estimates have also been developed by integrating multiple geophysical methods. For example, Fechner and Dietrich (1997) and Dietrich et al. (1998) used a combination of seismic and electric tomography to delineate major lithological units in a sedimentary aquifer. Tronicke et al. (2004) systematically investigated the potential of integrating crosshole GPR velocity and attenuation tomography to characterize highly heterogeneous sand and gravel aquifers. They found that this combination is a promising tool for delineating the major subsurface zonation as well as estimating hydrogeologic parameters within each zone. Figure 13.4 gives an example of such a zonal data integration (adapted from Tronicke et al., 2004). The crosshole tomographic GPR data set was gathered at the Boise Hydrogeophysical Research Site, Idaho, and first-arrival travel times and amplitudes were used to tomographically reconstruct the velocity and attenuation structure between two boreholes (Figures 13.4a and 13.4b). These two parameter fields were then integrated using *k*-means cluster analysis, a well-known unsupervised classification technique. Tronicke et al. (2004) conclude that the resulting zonal image of the interborehole plane (Figure 13.4c) outlines the main structural features visible in the two tomographic images and is consistent with well logs from the site. Well logs (such as neutron porosity and flowmeter logs) or other available information on the hydraulic properties (e.g., from pump or tracer tests) can then be used to develop a zonal hydrogeological model of the subsurface.

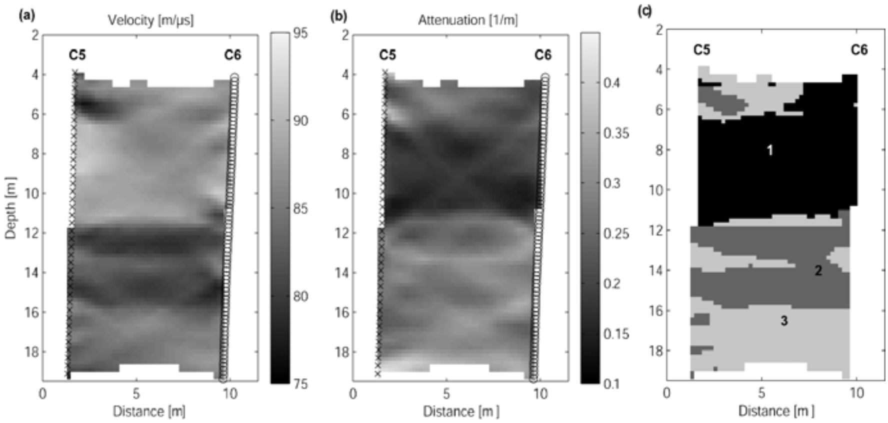

Figure 13.4. Example of integrating different crosshole tomographic parameter distributions into one zonal subsurface model (modified after Tronicke et al., 2004): (a) GPR velocity tomogram, (b) GPR attenuation tomogram, and (c) zonal model generated using cluster analysis. In (a) and (b), stars and circles denote transmitter and receiver positions in boreholes C5 and C6, respectively. In (c), numbers and gray scales represent three characteristic zones that can be identified using cluster analysis.

Estimating Aquifer Flow and Transport Parameters

There are a number of studies in the recent literature that focus on estimating hydrogeological parameters and their spatial distributions directly from geophysical measurements. Often, petrophysical relationships and models are used (as presented for example in Chapters 4 and 9 of this volume) to transform a resulting geophysical parameter into the hydrogeological parameter of interest. Hydrogeologic properties are most commonly estimated using crosshole geophysical methods, because it is difficult to resolve such properties with sufficient accuracy using current surface-based geophysical methods.

13.3.1 ESTIMATING HYDROGEOLOGICAL PROPERTIES

A significant effort over the last two decades has focused on estimating aquifers from the complementary nature of different types of data collected at multiple overlapping scales. Sediment cores provide information at the point scale, whereas pump- and slug-test data provide information in the vicinity of a well bore. Crosswell geophysical tomography provides dense information for a cross section between wells, whereas some surface geophysical data can provide three-dimensional information about the geometry of shallow lithologies. Measured tracer concentrations and changes in hydraulic heads during pumping events provide information about the average hydraulic properties between wells. Since the scale measured by each type of data is different but overlapping, combinations of these data types provide information that could not be obtained using any single data type alone. Several approaches have been used to combine such disparate datasets. Below, we review several approaches and give examples of how they have been used to estimate hydrogeological parameters in the saturated zone at the local scale.

13.3.1.1 *Geostatistical Methods*

Geostatistical methods can be used to combine diverse data types such as those obtained from geophysical and hydrogeologic data. These methods interpolate between available data points using weights that represent modeled spatial correlation structures and the uncertainty in the different measurement methods. Weights are generally assigned through a covariance matrix that incorporates the inferred spatial correlation of each variable and the interrelationships between variables, as described in Chapter 3 of this volume.

Several geostatistical methods that use surface seismic and GPR data sets to provide information about the heterogeneous structure of aquifers and reservoirs have been developed. The simplest approach is to *cokrige* the different data sets based on the inferred correlation structures of each variable and cross-correlation between datasets. The benefit of adding high-resolution soft seismic data to hard well-log data has been demonstrated in a number of studies. For example, Araktingi and Bashore (1992) cokriged three-dimensional surface-seismic-velocity estimates with porosity measurements, and found that even poor-quality seismic estimates provided information about reservoir properties. However, traditional cokriging cannot incorporate the likely nonlinear and non-unique relations between a hydrogeologic parameter of interest and the accompanying soft geophysical estimates.

Sequential Gaussian co-simulation (Deutsch and Journel, 1998) provides an additional geostatistical method for simulating hydraulic conductivity realizations based on hydraulic conductivity measurements (hard, or direct data) and geophysical attributes (soft, or indirect data). Sequential Gaussian co-simulation honors all estimated geophysical attributes, as well as the sample probability distribution and variograms of these attributes. One limitation of this approach is the reliance on a linear relation between soft and hard data (such as seismic slowness and hydraulic conductivity), which limits its application for many sites. For the Kesterson aquifer in California's San Joaquin Valley, Hyndman et al. (2000) found significant linear correlation between seismic slowness estimates obtained from crosshole seismic tomography and natural log hydraulic measurements from permeameter analysis of core samples and pump tests in the wells. Figure 13.5 is a log conductivity realization generated using sequential Gaussian co-simulation of *hard* hydraulic conductivity data, and *soft* seismic slowness estimates obtained from seven crosshole tomography planes for the site (modified from Hyndman et al., 2000). This study also demonstrated that the addition of crosswell seismic tomography data improved the accuracy of simulated tracer transport through the Kesterson aquifer. This example illustrates a simple approach for incorporating dense geophysical data and sparse measurement of the hydrogeologic properties of interest, in cases where reasonable correlation exists between these properties.

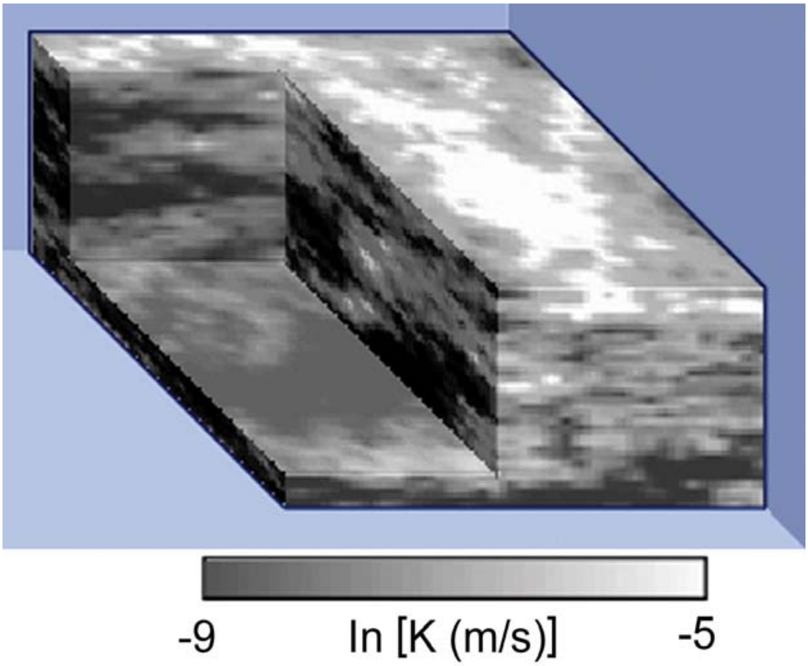

Figure 13.5. Realization of ln(K) obtained using sequential Gaussian co-simulation of crosswell seismic tomograms and local values of hydraulic conductivity at boreholes for the Kesterson site in California (modified after Hyndman et al., 2000)

13.3.1.2 *Bayesian Approaches*

Another suite of approaches for integrating geophysical and hydrogeological data involves Bayesian updating principles. These approaches develop prior estimates of hydraulic properties as described in Chapter 17 of this volume, and then update these prior estimates using more densely sampled geophysical data. The first step in the Bayesian estimation method is the development of a prior probability distribution function (pdf). This can be accomplished by (for example) interpolating the direct estimates of hydraulic conductivity from well bores using kriging (e.g., Deutsch and Journel, 1998). The second step is to estimate the joint distribution between the log of hydraulic conductivity and a geophysical parameter (such as seismic or GPR velocity) based on collocated data. This distribution is then used within Bayes' formula to update the prior pdf based on the estimated geophysical parameters, providing a posterior distribution. This inversion process is schematically shown in Figure 13.6 (modified from Hubbard et al., 2001) and is discussed in Chapter 17 of this volume.

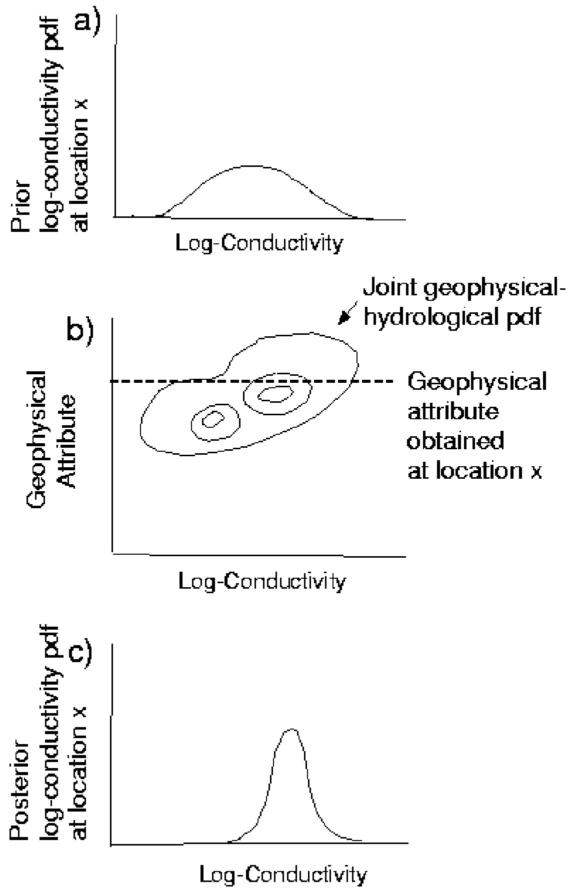

Figure 13.6. Schematic diagram of the Bayesian estimation approach: (a) example of a prior log K pdf for a point; (b) joint distribution of log hydraulic conductivity and a particular geophysical attribute such as GPR velocity; and (c) example of a posterior log (K) pdf obtained using the Bayes theorem to update a using b (modified after Hubbard et al., 2001)

This general approach was applied to estimate the log-hydraulic conductivity values at the US Department of Energy bacterial transport site near Oyster Point, Virginia (Hubbard et al., 2001). Chen et al. (2001) demonstrated that the addition of crosshole GPR tomograms reduced the estimation errors relative to the prior estimates, based on hydraulic conductivity data alone. Figure 13.7 (modified from Hubbard et al., 2001) illustrates the hydraulic conductivity estimates obtained using the Bayesian approach, along with an overlay of the hydraulic conductivity values estimated at a borehole using a flowmeter. As expected, geophysical information was most beneficial in the parameter estimation process far from locations where direct estimates of hydraulic conductivity existed. Hubbard et al. (2001) also examined tracer concentrations relative to the tomographic estimates and found that both spatial moments of the plume and the visual aspects of the project were reasonably consistent with the geophysical data.

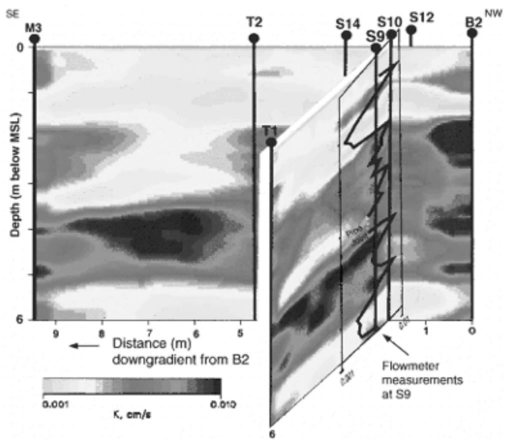

Figure 13.7. Estimated mean log (K) values estimated for the Oyster Point, VA, site, based on crosshole GPR tomograms and conductivity data obtained from borehole flowmeter tests, one of which is shown for well S9 (modified after Hubbard et al., 2001)

13.3.1.3 *Zonal Inversion Methods*

A different philosophy for combining geophysical and hydrogeologic data involves estimating the geometry of lithologic zones and the effective hydrogeologic properties for each zone that are consistent with geophysical, tracer, and hydraulic data sets. This philosophy was implemented in the split inversion method (SIM) (Hyndman et al., 1994), which co-inverts independently collected datasets (e.g., crosswell seismic travel times and tracer concentration histories) for the zonation of lithologies, effective hydraulic conductivity values for each zone, and an effective dispersivity for the region. The motivation for developing such an approach was that the combined analysis of crosswell geophysical data and tracer concentrations, which have independently sampled portions of the same environment, should provide better estimates of the geometry of subsurface lithologies and effective zonal properties than obtained using either data set alone. A particular advantage of this approach is that it does not rely on knowledge of the relationship between the geophysical attribute and the hydraulic parameter, although it assumes some relationship exists for large-scale lithologic zones. The relationship can be nonlinear and non-unique. For example, Hyndman et al. (1994) found that this approach could accurately identify the properties of two synthetic aquifers that had the same seismic response but different distributions of hydraulic conductivity.

Hyndman and Gorelick (1996) also applied the SIM to the Kesterson aquifer discussed in Sections 13.2 and 13.3.1.1 above. The seismic slowness was first estimated along the vertical planes between wells using seismic travel-time tomography (updated from zonal tomograms shown in Figure 13.3; the tomogram planes were below the white lines in Figure 13.8a). Sequential Gaussian simulation (Deutsch and Journal, 1998) was then used to develop three-dimensional conditional seismic slowness realizations (e.g., Figure 13.8a) for a region surrounding the tomograms, using the modeled correlation structure from the tomograms. The SIM approach was then used to split each slowness realization into lithologic classes (e.g., Figure 13.8b) and to estimate the effective hydraulic conductivity for each lithology as well as a regional dispersivity value.

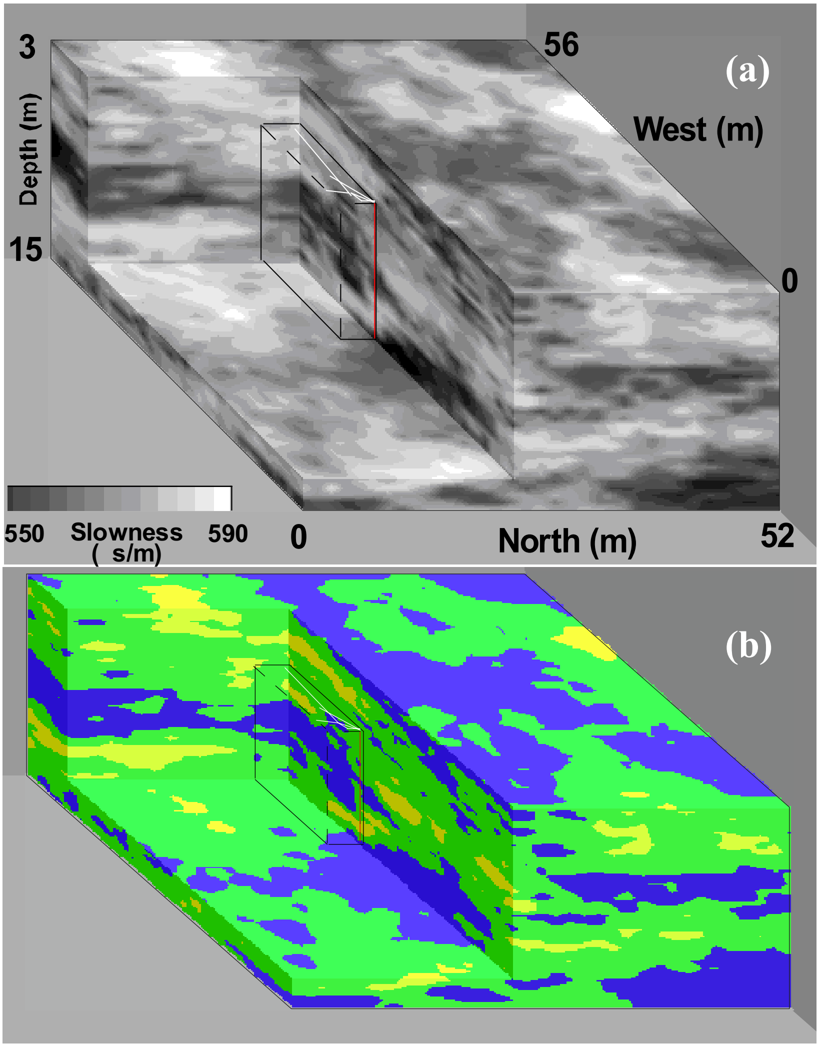

Figure 13.8. (a) Three-dimensional seismic slowness realization generated using sequential Gaussian simulation, which preserves slowness estimates and correlation structure from tomograms along planes below white lines. (b) Three-dimensional estimate of log hydraulic conductivity developed using the SIM. Hydraulic conductivity estimates are 1.4×10^{-4}, 3.6×10^{-4}, and 5×10^{-4} (m/s) for the black, dark gray and light gray zones respectively. Modified from Hyndman and Gorelick (1996).

The objective function of this inversion was to minimize the squared residual between observed and simulated tracer arrival-time quantiles, and drawdown during the forced gradient tracer test. This study again demonstrated the value of seismic tomography for estimating the hydraulic conductivity structure of a heterogeneous aquifer. The tomography estimates provided information about the geometry of lithologic zones and the correlation structure of the aquifer lithologies. Drawdown values measured during the tracer test provided critical information about the average regional hydraulic conductivity at the site, and tracer concentration data provided information about the continuity of hydraulic conductivity across the test region.

The parameter estimation approaches described above illustrate the potential of geophysical information to increase the resolution of hydraulic property estimates. Changes in subsurface lithologies at some scales should commonly change both geophysical and hydraulic properties—consequently, combining these diverse datasets provides better estimates than can be obtained with any single dataset.

13.3.1.4 *Theoretical Methods*

Yamamoto et al. (1995) employed crosshole seismic tomography to estimate permeability within a limestone aquifer. They used tomographic surveys repeated for different signal frequencies to obtain velocity-frequency dispersion data. Based on the Biot-squirt flow theory, resulting dispersion data were used to qualitatively estimate permeability values, which compared well to permeability values determined from pumping test data. Yamamoto (2001) also developed a procedure to quantitatively estimate the distribution of porosity, shear strength, and permeability from seismic data. This technique was applied to crosshole seismic data, and the results were compared to available logging data. It gave reasonable agreement in some cases, whereas only qualitative agreement was found in other cases.

13.3.2 ESTIMATING SPATIAL CORRELATION PARAMETERS USING GEOPHYSICAL DATA

Several studies have recognized that geophysical methods can be used to estimate the spatial correlation structure of hydraulic properties. Such spatial correlation parameters are used to develop three-dimensional estimates of aquifer parameters and are needed to create stochastic flow and transport models. However, these parameters are generally difficult to estimate in the horizontal direction because of inadequate sampling with typical well and core data. Geophysical data can provide densely sampled estimates in the horizontal direction and can thus improve estimates of spatial correlation parameters. Rea and Knight (1998) used surface GPR to estimate correlation lengths and the maximum correlation direction for a gravel pit site in British Columbia, Canada. They then digitized images of a gravel pit vertical face and compared correlation lengths from this image to the geophysical estimates, and found that the results were similar. Tercier et al. (2000) found significant differences in the correlation structures obtained from GPR reflection images of deltaic and barrier-spit depositional environments. They concluded that the correlation structure of GPR images can be closely related to the processes that formed the imaged geological section, and thus this information can be useful for characterizing subsurface spatial heterogeneity. More recently, Oldenborger et al. (2003) used a similar approach in a gravel pit with comparisons to hydraulic conductivity measured on cores and found that the correlation structure of stacked velocities from a common midpoint (CMP) survey compared reasonably well with those from the measured hydraulic conductivity field. In contrast, they found that geostatistical analyses of the more common reflection images provided quite different estimates of correlation parameters. Using crosshole tomographic data, Hubbard et al. (1999) investigated the importance of considering the scale of the measurement relative to the scale of heterogeneity when using geophysical data (in this case, seismic and radar tomographic data) to obtain structural correlation parameters.

13.4 Mapping Temporal Changes

Perhaps the most exciting advance in hydrogeophysics is the ability of geophysical methods to provide time-lapse images of tracers moving through the subsurface. Such approaches provide the potential to overcome the unknown and non-unique relations between geophysical and hydrologic properties discussed in the introduction to this chapter. Methods that are able to geophysically image the movement of fluids or solutes can be more directly related to the hydrogeologic properties of interest than passive imaging methods.

13.4.1 IMAGING CHANGES IN WATER TABLE ELEVATION

Conventionally, the hydraulic response of an aquifer is measured in a series of monitoring wells during a pump test. Often, the number of observation wells is limited, and their spatial distribution is not sufficient to study the response of the experiment in detail. In this section, we explore the potential of seismic and GPR methods to provide high-resolution estimates of water table fluctuations. Electrical Resistance Tomography (ERT) and other electrical methods can also be used for this type of analysis, as discussed in Chapter 14 of this volume.

Birkelo et al. (1987) reported the use of time-lapse seismic reflection data, gathered during a pumping test, for investigating an unconfined alluvial aquifer. They demonstrated that seismic reflection data can image the top of shallow ($<$2.5 m) saturated zones, but that there was little change in the seismic response during eight days of pumping, even though drawdowns of several meters were measured in nearby wells. They speculated that a near-surface clay layer inhibited drainage in the upper part of the studied aquifer. Baker et al. (2000) used surface seismic reflection data to monitor seasonal water table fluctuations in an alluvial aquifer, with a reported accuracy of ±12 cm. They concluded that detailed seismic velocity information, which can be obtained from common midpoint surveys, was critical in providing accurate estimates of water table depths from seismic reflection data.

Endres et al. (2000) investigated the potential of time-lapse surface GPR reflection data to map the drawdown associated with a pumping test carried out at the Canadian Forces Base (CFB) test site in Borden, Ontario. The aquifer at this site is composed of clean, well-sorted, medium- to fine-grained Pleistocene sand. They observed a reflection in the transition zone between the overlying residually saturated material and the capillary fringe below, rather than at the water table depth. They used the arrival-time delay of this reflection to infer the drawdown during the pumping test. Figure 13.9 shows distance- and time-drawdown curves based on GPR and piezometer data collected during this experiment. The comparison shows that the drawdown estimated from GPR is both smaller and delayed compared to the drawdown directly measured from piezometers. Endres et al. (2000) interpreted the difference to result from an increase of the combined thickness of the transition zone and capillary fringe during the pump test. They concluded that GPR-derived information can be useful in imaging a pumping test, but that there is a need for future research. Bentley and Trenholm (2002) also investigated the accuracy of GPR for estimating water table elevations in unconsolidated sediments in Canada. They used theoretical models and field data to quantify sources of uncertainty for estimating water table elevations (uncertainty in the velocity model, uncertainty in surface elevation, and uncertainty in the capillary fringe height) using GPR frequencies of 100 and 200 MHz. They concluded that the shallow water table elevation can be estimated with an accuracy of roughly 0.2 m in their particular test environment. Extensive discussions of water table mapping using GPR data are given in Chapter 14 of this volume.

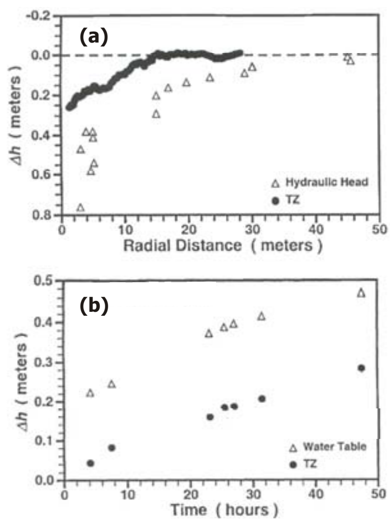

Figure 13.9. Comparison of drawdown during a pumping experiment measured with piezometers and GPR (modified after Endres et al., 2000): (a) Distance-drawdown after 23 hours determined from hydraulic head measurements and from transition zone reflection times (TZ); (b) Time-drawdown curves from hydraulic head measurements and from transition zone reflection times (TZ) for a radial distance of 5 m.

In another interesting experiment, Tsoflias et al. (2001) studied the GPR response during a pumping test in a fractured aquifer. First, they employed forward electromagnetic modeling of thin layers (simulating the fractures) to investigate the GPR waveform changes associated with changes in fracture saturation. GPR surveys carried out before and during a pump test provided data that were consistent with piezometric head measurements. Using these data, Tsoflias et al. (2001) interpreted a drainage pattern for a prominent fracture. They concluded that GPR surveying combined with hydraulic data can provide improved understanding of fluid flow within fractured formations at the local scale.

The studies discussed above indicate that geophysical data can provide insight into variations in water table and capillary fringe elevations during pumping tests or natural seasonal changes. However, these studies also indicate that additional research is needed to improve both the resolution of the estimates and the interpretation of measured changes. Additional examples of the use of geophysical methods for mapping the water table are given in Chapter 14 of this volume.

13.4.2 PLUME MAPPING AND DYNAMIC IMAGING

There is a significant need for new methods that can either infer contaminant concentrations across plumes or remotely image the size and shape of contaminant plumes. Even limited direct characterization of plumes is extremely expensive. Without remote technology, contaminant plumes are always undersampled. New remote plume imaging methods could reduce the cost of contaminant remediation systems, because they could be placed in locations that would maximize the contaminant treatment with the minimum installation and operation costs.

A number of controlled experiments at the laboratory or field scale indicate the potential of geophysical techniques, such as electric and electromagnetic methods, to detect and map nonaqueous phase liquids (NAPLs) and other contaminants within the subsurface (e.g., Olhoeft, 1992; Brewster and Annan, 1994; Endres and Redman, 1996; Grumman and Daniels, 1996; Sandberg et al., 2002). Because of the complexity and heterogeneity of near-surface environments, it is especially difficult to relate a single geophysical parameter (e.g., electrical resistivity or GPR reflectivity) to a specific contaminant. Additional information can be provided through the use of multiple geophysical techniques constrained by various borehole-based data, as for example presented by Atekwana et al. (2000). Deeds and Bradford (2002) report the direct detection of light non-aqueous phase liquid (LNAPL) using advanced processing techniques for multi-offset GPR data. They used detailed velocity information and AVO (amplitude versus offset) analysis assisted by systematic coring.

Another approach for detecting and mapping contamination plumes is to observe subsurface changes with time. In the Borden experiment (Greenhouse et al., 1993), a controlled DNAPL (dense NAPL) release was monitored with various geophysical techniques. In this experiment, 770 L of perchloroethylene (PCE) were released over a 70-hour period into a 9×9×3.3 m cell containing medium- to fine-grained sand. Brewster and Annan (1994) present the results of detecting and monitoring this release with 200 MHz GPR. Under these ideal conditions, it was possible to relate certain reflectors to plume movement. Brewster and Annan (1994) also found that lateral and/or temporal variations in GPR velocity from CMP gathers can be helpful in reliably interpreting the data. The referenced publications and other recent studies indicate that in uncontrolled field settings, assisting information (e.g., direct sampling by systematic coring) is indispensable for obtaining a reliable link between geophysical data and contaminant plume detection. Identifying DNAPL pools at contaminated sites is a daunting task, because it can be difficult to separate variations in fluid properties from changes in subsurface geology, unless the site is already well characterized.

Dynamic imaging of changes in fluid properties is another exciting area of hydrogeophysics. Many of the traditional problems of interpreting geophysical images in terms of hydraulic properties can be reduced or eliminated in this class of problems. The potential of electrical methods was recognized decades ago, especially to monitor the movement of saline tracers and to derive hydrological parameters such as groundwater velocity (Fried, 1975; White, 1988; Bevc and Morrison, 1991; White 1994). Ramirez et al. (1993) discussed an experiment in which electrical resistance tomography (ERT) was used to image a plume of injected steam designed to remediate volatile organic contaminants at the Lawrence Livermore National Laboratory site. They found that ERT did a reasonable job of imaging the measured changes in sediment resistivity, and they also found that the steam flood was likely constrained by a gravel layer across the site. More recently, developments in inversion techniques allow tomographic imaging of the tracer plume and its development with time. This has increased the popularity of dynamic electrical imaging. Good examples of this technique for various applications include Slater et al. (1997), Daily and Ramirez (2000), and Kemna et al. (2002).

In a carefully designed field experiment, the background conditions can be measured before a tracer is injected, and then a series of differenced geophysical images can be used to image the moving tracer plume. One of the keys to this type of experiment is choosing tracer concentrations that provide enough geophysical contrast while still allowing some energy to propagate through the tracer plume. Details of the design of this type of test and some preliminary results for the dynamic imaging of a bromide salt tracer plume injected into the Boise Hydrogeophysical Research Site, Idaho, are given by Barrash et al. (2003) and Goldstein et al. (2003).

Figure 13.10 illustrates the results of a 3-D saline tracer experiment monitored using ERT (adapted from Mohrlock and Dietrich, 2001). In a gravel- and sand-dominated aquifer located in the Rhine Valley in southwest Germany, these authors used arrays of borehole electrodes installed in six boreholes. In a long-term experiment (i.e., over a period of several weeks), the use of borehole electrodes improved data quality, because these measurements were less affected by the significant near-ground-surface resistivity variations, e.g., caused by changes in water content. Using a 3-D inversion technique and relating certain iso-surfaces of electrical resistivity to the tracer plume, Mohrlock and Dietrich (2001) were able to generate 3-D images of the tracer plume and its movement with time, as illustrated in Figure 13.10.

Day-Lewis et al. (2002) illustrated the utility of dynamic tracer imaging using time-lapse crosshole GPR tomography. Using a synthetic GPR data set, the authors developed a sequential inversion approach to image multiple time slices of an electrically conductive tracer moving through a fracture zone. Day-Lewis et al. (2003) then applied this approach to evaluate a saline tracer test at the U.S. Geological Survey Fractured Rock Hydrology Research Site in Grafton County, New Hampshire. They found that their sequential time-lapse inversion allowed them to identify a preferential flowpath through an identified fracture and estimate the time of peak tracer arrival at the geophysically imaged planes. Such field tests need to be carefully designed to avoid temporal aliasing, which occurs when the time step of the GPR acquisition is greater than the time step of the tracer plume movement.

Time-lapse imaging methods, such as presented in the cases discussed above, provide the potential for significant insight into flow and transport dynamics in heterogeneous aquifers. Water levels and solute concentrations can only be measured at a limited number of well points across an aquifer, whereas geophysical methods have the potential to provide 2- to 3-dimensional estimates of solute concentrations through time between such wells.

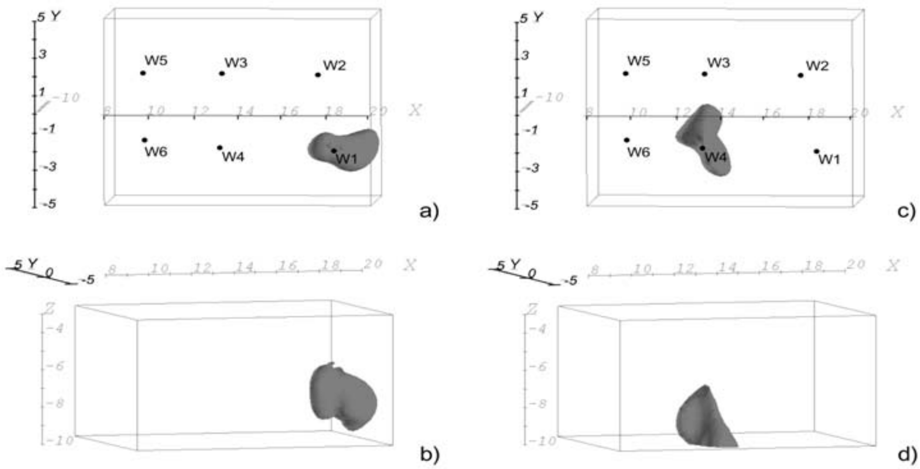

Figure 13.10. Three-dimensional electrical imaging of a salt tracer plume and its propagation in a sand- and gravel-dominated aquifer (adapted from Mohrloch and Dietrich, 2001). The images show selected iso-surfaces of changes in electrical resistivity for different times and perspectives: (a) Top view after twelve days of tracer propagation; (b) Side view after twelve days; (c) Top view after 24 days; and (d) Side view after 24 days. All axes dimensions are in meters.

13.5 Aquifer Analog Studies

Outcrop analog approaches have been applied mainly in the field of petroleum exploration to characterize the properties of petroleum reservoirs (e.g., Miall, 1988). The concept has also been used in aquifer studies to investigate geometries and hydraulic properties of various sedimentological units (e.g., Macfarlane et al., 1994; Heinz et al., 2003). Such analog approaches involve the detailed investigation of accessible outcrops of a representative sedimentary formation. It is assumed that the geometric and physical parameter distributions are comparable to those of the inaccessible aquifer. Such models can then be used to simulate geophysical measurements (Dietrich et al., 1998; Kowalsky et all, 2001) as well as groundwater flow and transport (Whittaker and Teutsch, 1999) on an analog model of an aquifer that is as close as possible to reality.

Figure 13.11 illustrates an analog study presented by Tronicke et al. (2002). The authors carried out geophysical measurements (GPR reflection surveying, crosshole GPR tomography, and natural gamma activity logging) in braided stream deposits. Their test site was located in a gravel pit in the upper Rhine Valley of southwest Germany. After geophysical surveying, they excavated their test site and photographed the outcrop plane corresponding to their geophysical measurement plane, using a special wide-angle lens to ensure that the photographs were free of distortion. The digitized photographs were then interpreted in terms of different lithologies, resulting in a map of the 2-D lithofacies distribution in the surveyed plane. They found reasonable agreement between their structural interpretation of the combined geophysical results and the main sedimentary units observed in the outcrop. In addition, they transformed the obtained lithofacies distribution into hydraulic conductivity and porosity values using the procedure of Klingbeil et al. (1999). This enabled an impact analysis of different structures detected by geophysical tools using a series of groundwater flow and transport models. Tronicke et al. (2002) concluded that the incorporation of integrated high-resolution geophysical information improved the hydraulic characterization of the heterogeneous deposit.

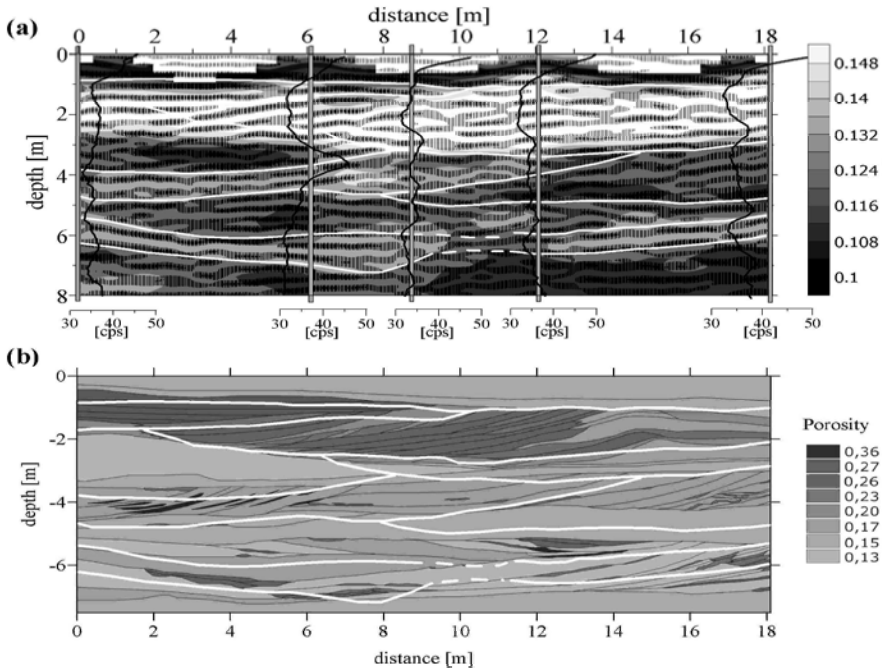

Figure 13.11. Example of a detailed aquifer analog study for evaluating geophysical techniques and their potential in braided stream deposits (modified after Tronicke et al., 2002): (a) Combined visualization of GPR reflection image, GPR velocity distribution tomographically reconstructed from three crosshole surveys, and natural gamma activity logging (borehole locations are denoted by grey rectangles); (b) Lithofacies distribution converted into porosities in the geophysical measuring plane interpreted from a photograph taken after excavation. The white lines represent a structural interpretation based on all shown geophysical results. Note the reasonable agreement between the structures detected by geophysical techniques and the main sedimentary units in (b).

13.6 Concluding Remarks

The case studies presented in this chapter illustrate the benefit of using geophysical techniques for a variety of subsurface characterization and monitoring objectives within saturated aquifers at the local scale. These objectives include delineation of structural aquifer features, direct estimation of hydraulic relevant parameters, integrated hydrogeophysical approaches to characterize flow and transport parameters, and dynamic imaging of variations in tracer or contaminant concentrations. The ability of geophysical methods to provide densely sampled information, relative to traditional hydrogeological methods, makes them attractive for subsurface characterization at the local scale, such as for investigating a contaminated site. While some tasks involve standard applications of geophysical methods (e.g., mapping depth to bedrock), other problems require novel techniques and analysis methods that are still in the development stages (e.g., relating and integrating geophysical and hydrological data). Integration of various soft geophysical data and various hard data, such as provided by borehole-based hydrogeological methods, may help to reduce uncertainties and non-uniqueness during processing and data analysis, and may help to generate more reliable flow and transport models at specific sites. The presented studies show the benefit of integrated hydrologic and geophysical approaches. One of the most exciting areas of research is the emerging field of dynamic imaging, which allows for passive contaminant site monitoring, active plume migration imaging, and more accurate hydraulic property estimation than with static measurements.

References

Araktingi, U.G., and W.M. Bashore, Effects of properties in seismic data on reservoir characterization and consequent fluid flow predictions when integrated with well logs, Paper presented at 67th Annual SPE Conference, Soc. Pet. Eng., Washington, D.C., Oct. 4–7, 1992.

Atekwana, E.A., W.A. Sauck, and D.D. Werkema, Investigations of geoelectrical signatures at a hydrocarbon contaminated site, *Journal of Applied Geophysics*, *44*, 167–180, 2000.

Baker, G.S., D.W. Steeples, C. Schmeissner, and K.T. Spikes, Ultrashallow seismic reflection monitoring of seasonal fluctuations in the water table, *Environmental and Engineering Geoscience*, *6*(3), 271–277, 2000.

Baines, D., D.G. Smith, D. Froese, P. Bauman, and G. Nimeck, Electrical resistivity ground imaging (ERGI): a new tool for mapping the lithology and geometry of channe-belts and valley-fills, *Sedimentology, 49*, 441–449, 2002.

Barrash, W., M.D. Knoll, D.W. Hyndman, T. Clemo, E.C. Reboulet, and E.M. Hausrath, Tracer/Time-Lapse Radar Imaging Test at the Boise Hydrogeophysical Research Site, In: *Proceedings of SAGEEP03, The Symposium on the Application of Geophysics to Engineering and Environmental Problems*, pp. 163–174, San Antonio, TX, 2003.

Bentley, L.R., and N.M. Trenholm, The accuracy of water table elevation estimates determined from ground penetrating radar data, *Journal of Environmental and Engineering Geophysics*, *7*(1), 37–53, 2002.

Beres, M., and F.P. Haeni, Application of ground-penetrating-radar methods in hydrogeologic studies, *Ground Water*, *29*(3), 375–387, 1991.

Beres, M., A.G. Green, P. Huggenberger, and H. Horstmeyer, Mapping the architecture of glaciofluvial sediments with three-dimensional georadar, *Geology*, *23*(12), 1087–1090, 1995.

Bevc, D., and H.F. Morrison, Borehole-to-surface electrical monitoring of a salt water injection experiment, *Geophysics*, *56*, 769–777, 1991.

Birkelo, B.A., D.W. Steeples, R.D. Miller, and M. Sophocleous, Seismic reflection study of a shallow aquifer during a pumping test, *Ground Water*, *25*(6), 703–709, 1987.
Bourbie, T., O. Coussy, and B. Zinszner, *Acoustics of Porous Media*, Gulf Publishing Company, Houston, 1987.
Brewster, M.L., and A.P. Annan, Ground-penetrating radar monitoring of a controlled DNAPL release: 200 MHz radar, *Geophysics*, *59*(8), 1211–1221, 1994.
Büker, F., A.G. Green, and H. Horstmeyer, 3-D high-resolution reflection seismic imaging of unconsolidated glacial and glaciolacustrine sediments: Processing and interpretation, *Geophysics*, *65*(1), 18–34, 2000.
Chen, J., S. Hubbard, and Y. Rubin, Estimating hydraulic conductivity at the South Oyster Site from geophysical tomographic data using Bayesian techniques based on the normal regression model, *Water Resour. Res.*, *37*(6), 1603–1613, 2001.
Daily, W.D., and A.L. Ramirez, Electrical imaging of engineered hydraulic barriers, *Geophysics*, *65*(1), 83–94, 2000.
Day-Lewis, F.D., J.M. Harris, and S.M. Gorelick, Time-lapse inversion of crosswell radar data, *Geophysics*, *67*(6), 1740–1752, 2002.
Day-Lewis, F.D., J.W. Lane, Jr., J.M. Harris, and S.M. Gorelick, Time-lapse imaging of saline-tracer transport in fractured rock using difference-attenuation radar tomography, *Water Resour. Res., 39*(10), *1290,* 10.1029/ 2002WR001722, 2003
Deeds, J., and J. Bradford, Characterization of an aquitard and direct detection of LNAPL at Hill Air Force Base using GPR AVO and migration velocity analyses, In: *Ninth International Conference on Ground Penetrating Radar (GPR 2002)*, edited by S. Koppenjan, and H. Lee, SPIE, 4758, pp. 323–329, Santa Barbara, California, 2002.
Deutsch, C.V., and A.G. Journel, *GSLIB: Geostatistical Software Library and User's Guide*, Oxford University Press, 1998.
Dietrich, P., T. Fechner, J. Whittaker, and G. Teutsch, An integrated hydrogeophysical approach to subsurface characterization, In: *Groundwater Quality: Remediation and Protection*, edited by M. Herbert, and K. Kovar, pp. 513–519, IAHS Publ., 250, Tübingen, Germany, 1998.
Dvorkin, J., G. Mavko, and A. Nur, Squirt flow in fully saturated rocks, *Geophysics*, *60*(1), 97–107, 1995.
Endres, A.L., W.P. Clement, and D.L. Rudolph, Ground penetrating radar imaging of an aquifer during a pumping test, *Ground Water*, *38*(4), 566–576, 2000.
Fechner, T., and P. Dietrich, Lithological inversion of tomographic data, In: *3rd Ann. Mtg., Environ. and Eng. Geophys. Soc., Euro. Section*, pp. 355–358, Aarhus, Denmark, 1997.
Fried, J.J., *Groundwater Pollution: Developments in Water Science 4*, Elsevier, 1975.
Goldstein, S.E., T.C. Johnson, M.D. Knoll, W. Barrash, and W.P. Clement, Borehole radar attenuation-difference tomography during the tracer/time-lapse test at the Boise Hydrogeophysical Research Site, In: *Proceedings of SAGEEP03, The Symposium on the Application of Geophysics to Engineering and Environmental Problems*, pp. 147–162, San Antonio, TX, 2003.
Greenhouse, J., M. Brewster, G. Schneider, J.D. Redman, A.P. Anna, G.R. Olhoeft, J. Lucius, K. Sander, and A. Mazzella, Geophysics and solvents: The Borden Experiment, *The Leading Edge of Exploration*, *12*, 261–267, 1993.
Grumman, D.L., and J.J. Daniels, Experiments on the detection of organic contaminants in the vadose zone, *Journal of Environmental and Engineering Geophysics*, 0(1), 31–38, 1995.
Heinz, J., S. Kleineidam, G. Teutsch, and T. Aigner, Heterogeneity patterns of Quaternary glaciofluvial gravel bodies (SW-Germany): application to hydrogeology, *Sedimentary Geology*, *158*, 1–23, 2003.
Hubbard, S.S., J. Chen, J.E. Peterson, E.L. Majer, K.H. Williams, D.J. Swift, B. Mailloux, and Y. Rubin, Hydrogeological characterization of the South Oyster Bacterial Transport Site using geophysical data, *Water Resour. Res.*, *37*(10), 2431–2456, 2001.
Hubbard, S.S., Y. Rubin, and E. Majer, Spatial correlation structure estimation using geophysical and hydrogeological data, *Water Resour. Res., 35*, 1809–1825, 1999.
Huggenberger, P., Radar facies: Recognition of facies patterns and heterogeneities within Pleistocene Rhine gravels, NE Switzerland, In: *Geological Society Special Publications No 75*, pp. 163–176, 1993.
Hyndman, D.W., and S.M. Gorelick, Estimating lithologic and transport properties in three dimensions using seismic and tracer data, *Water Resour. Res., 32*(9), 2659–2670, 1996.
Hyndman, D.W., J.M. Harris, and S.M. Gorelick, Coupled seismic and tracer test inversion for aquifer property characterization, *Water Resour. Res., 30*(7), 1965–1977, 1994.
Hyndman, D.W., and J.M. Harris, Traveltime inversion for the geometry of aquifer lithologies, *Geophysics, 61*(6), 1996.
Hyndman, D.W., S.M. Gorelick, and J.M. Harris, Inferring the relationship between seismic slowness and hydraulic conductivity in heterogeneous aquifers, *Water Resour. Res., 36*(8), 2121–2132, 2000.

Jarvis K.D. and R.J. Knight, Aquifer heterogeneity from SH-wave seismic impedance inversion, *Geophysics, 67*(5), 1548–1557, 2002.

Kemna, A., J. Vanderborght, B. Kulessa, and H. Vereecken, Imaging and characterization of subsurface solute transport using electrical resistivity tomography (ERT) and equivalent transport models, *Journal of Hydrology*, *267*(3–4), 125–146, 2002.

Kick, J.F., Depth to bedrock using gravimetry, *The Leading Edge of Exploration*, *4*(4), 38–42, 1985.

Klingbeil, R., S. Kleineidam, U. Asprion, T. Aigner, and G. Teutsch, Relating lithofacies to hydrofacies: Outcrop-based hydrogeological characterization of Quaternary gravel deposits, *Sedimentary Geology*, *129*(3–4), 299–310, 1999.

Kowalsky, M.B., Dietrich, P., Teutsch, G., and Y. Rubin, Forward modeling of GPR data usingdigitized outcrop images and multiple scenarios of water saturation, Water Resour. Res., 37(6), 1615-1625, 2001.

Lesmes, D.P., S.M. Decker, and D.C. Roy, A multiscale radar-stratigraphic analysis of fluvial aquifer heterogeneity, *Geophysics*, *67*(5), 1452–1464, 2002.

Lunt, I.A., J.S. Bridge, and R.S. Tye, Development of a 3-D depositional model of braided river gravels and sands to improve aquifer characterization, In: *Aquifer Characterization*, SEPM Concepts in Paleontology and Sedimentology Series, J.S. Bridge and D.W Hyndman, eds., 2003 (in press).

Macfarlane, P.A., J.H. Doveton, H.R. Feldmann, J.J. Butler, J.M.J. Combes, and D.R. Collins, Aquifer/aquitard units of the Dakota aquifer system in Kansas: Methods of delineation and sedimentary architecture effects on groundwater flow and flow properties, *Journal of Sedimentary Research*, *B 64/4*, 464–480, 1994.

McMechan, G.A., G.C. Gaynor, and R.B. Szerbiak, Use of ground-penetrating radar for 3-D sedimentological characterization of clastic reservoir analogs, *Geophysics*, *62*(3), 786–796, 1997.

Miller, R.D., D.W. Steeples, R.W. Hill, and B.L. Gaddis, Identifying intra-alluvial and bedrock structures shallower than 30 meters using seismic reflection techniques, In: *Geotechnical and Environmental Geophysics, Volume 2: Environmental and Groundwater*, edited by S. Ward, pp. 75–88, Society of Exploration Geophysics, 1990.

Miall, A.D., Reservoir heterogeneities in fluvial sandstones: Lessons from outcrop studies, *AAPG Bulletin*, *72*(6), 682–697, 1988.

Mohrlok, U. and Dietrich, P., Exploration of preferential transport paths using geoelectrical salt tracer tests. In: Field Screening Europe 2001—Proceedings of the Second International Conference on Strategies and Techniques for the Investigation and Monitoring of Contaminated Sites, W. Breh, J. Gottlieb, H. Hötzl, F. Kern, T. Liesch, and R. Niessner, eds., pp. 327–330, 2001.

Nitsche, F.O., A.G. Green, H. Horstmeyer, and F. Büker, Late Quaternary depositional history of the Reuss delta, Switzerland: Constraints from high-resolution seismic reflection and georadar surveys, *Journal of Quaternary Science*, *17*(2), 131–143, 2002.

Oldenborger, G.A., R.A. Schincariol, and L. Mansinha, Radar determination of the spatial structure of hydraulic conductivity, *Ground Water*, *41*(1), 24–32, 2003.

Olhoeft, G.R., Geophysical detection of hydrocarbon and organic chemical contaminants, In: *Proceedings of SAGEEP92, The Symposium on the Application of Geophysics to Engineering and Environmental Problems*, pp. 587–595, Oakbrook, IL, 1992.

Pellerin, L., Application of electrical and electromagnetic methods for environmental and geotechnical investigations, *Surveys in Geophysics*, *23*, 101–132, 2002.

Ramirez, A.L., W.D. Daily, D. Labrecque, E. Owen, and D. Chesnut, Monitoring an underground steam injection process using electrical-resistance tomography, *Water Resour. Res.*, *29*(1), 73–87, 1993.

Rea, J., and R. Knight, Geostatistical analysis of ground-penetrating radar data: A means of describing spatial variation in the subsurface, *Water Resour. Res.*, *34*(3), 329–339, 1998.

Regli C., P. Huggenberger, and M. Rauber, Interpretation of drill core and georadar data of coarse gravel deposits, *Journal of Hydrology, 255*(1–4), 234–252, 2002.

Sangree, J.M., and J.M. Widmier, Interpretation of depositional facies from seismic data, *Geophysics*, *44*, 131–160, 1979.

Sandberg, S.K., L.D. Slater, and R. Versteeg, An integrated geophysical investigation of the hydrogeology of an anisotropic unconfined aquifer, *Journal of Hydrology, 267*(3–4), 227–243, 2002.

Slater, L., A. Binley, and D. Brown, Electrical imaging of fractures using ground-water salinity change, *Ground Water*, *35*, 436–442, 1997.

Smith, D.G., and H.M. Jol, Ground-penetrating radar investigation of a Lake Bonneville Delta, Provo level, Brigham City, Utah, *Geology*, *20*(12), 1083–1086, 1992.

Tercier, P., R. Knight, and H. Jol, A comparison of the correlation structure in GPR images of deltaic and barrier-spit depositional environments, *Geophysics*, *65*(4), 1142–1153, 2000.

Tronicke, J., N. Blindow, R. Groß, and M.A. Lange, Joint application of surface electrical resistivity- and GPR-measurements for groundwater exploration on the island of Spiekeroog, northern Germany, *Journal of Hydrology*, *223*(1–2), 44–53, 1999.

Tronicke, J., P. Dietrich, U. Wahlig, and E. Appel, Integrating surface georadar and crosshole radar tomography: A validation experiment in braided stream deposits, *Geophysics*, *67*(5), 1495–1504, 2002.

Tronicke, J., K. Holliger, W. Barrash, M.D. Knoll, 2004, Multivariate analysis of crosshole georadar velocity and attenuation tomograms for aquifer zonation, *Water Resour. Res., 40(1), W01519,* 10.1029/2003WR002031.

Tsoflias, G.P., T. Halihan, and J.M. Sharp, Monitoring pumping test response in a fractured aquifer using ground-penetrating radar, *Water Resour. Res.*, *37*(5), 1221–1229, 2001.

van Overmeeren, R.A., Radar facies of unconsolidated sediments in The Netherlands: A radar stratigraphy interpretation method for hydrogeology, *Journal of Applied Geophysics*, *40*, 1–18, 1998.

Ward, S. H., editor, Geotechnical and Environmental Geophysics, Volumes I-III, Investigations in Geophysics #5, Society of Exploration Geophysicists, 1990.

White, P.A., Measurement of groundwater parameters using salt-water injection and surface resistivity, *Ground Water*, *26*, 179–186, 1988.

White, P.A., Electrode arrays for measuring groundwater flow direction and velocity, *Geophysics*, *59*(2), 192–201, 1994.

Whittaker, J., and G. Teutsch, Numerical simulation of subsurface characterization methods: application to a natural aquifer analogue, *Advances in Water Resources*, *22*(8), 819–829, 1999.

Yamamoto, T., T. Nye, and M. Kuru, Imaging the permeability structure of a limestone aquifer by crosswell acoustic tomography, *Geophysics*, *60*, 1634–1645, 1995.

Yamamoto, T., Imaging the permeability structure within the near-surface sediments by acoustic crosswell tomography, *Journal of Applied Geophysics*, *47*, 1–11, 2001.

Yaramanci, U., G. Lange, and M. Hertrich, Aquifer characterisation using surface NMR jointly with other geophysical techniques at the Nauen/Berlin test site, *Journal of Applied Geophysics*, *50*, 47–65, 2002.

Young, R.A., and Y. Sun, 3-D ground-penetrating radar imaging of a shallow aquifer at Hill Air Force Base, Utah, *Journal of Environmental and Engineering Geophysics*, *1*(2), 97–108, 1996.